Organic Process Research & Development

Article

pubs.acs.org/OPRD

Utilization of ReactIR in Fit for Purpose Process Enablement

Shane A. Eisenbeis,* Raymond Chen, Ming Kang, Mark Barrila, and Richard Buzon

Pharmaceutical Sciences—Research API, Pfizer Global Research & Development Eastern Point Road, Groton, Connecticut 06340, United States

ABSTRACT: An efficient four-step synthesis of **1** is described in which utilization of ReactIR was key to efficient processing and reaction monitoring. Key chemical steps included (i) nucleophilic aromatic substitution, iron reduction of aromatic nitro group to aniline, (ii) decarboxylation, and (iii) ester formation.

INTRODUCTION

We recently required multikilogram quantities of amide (**1**, Figure 1) for use in toxicological studies. Several challenges

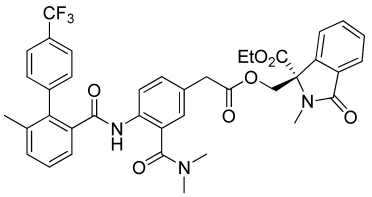

1

Figure 1. Structure of amide (**1**).

were associated with the target, including formation of the chiral center, process monitoring at elevated temperatures, and the final form of **1**.

The original preparation of **1** (Scheme 1) was conceptually straightforward but suffered from a relatively lengthy linear sequence of reactions, multiple solvent systems, and the inability to isolate final amide (**1**) in a usable form. The route provided access to 10 g quantities of **1**, but with modest overall yields (~23%), it became clear that further scale-up would require significant process enabling.

DISCUSSION

Synthesis of (10). Initial efforts focused on a more convergent process, eliminating multiple catalyst charges, solvents, and unnecessary protection schemes. The processing was broken down into three components which would serve as key building blocks.

Diethyl malonate was selected over dimethyl malonate for the nucleophilic aromatic substitution, providing a significantly cleaner conversion of (**2**) to (**12**) in 2-MeTHF (Scheme 2). Reduction of crude nitrobenzene (**12**) to aniline (**13**) was achieved under Fe−HOAc conditions.[1] This resolved the issue of multiple catalyst charging, thus significantly improving processing safety. The aniline (**13**) was readily isolated from the mixture as a solid which could be further purified by triturating in heptanes if needed. This process was outsourced to multiple vendors who successfully prepared **13** to support the manufacturing campaign described later herein.

Scheme 1. Original synthesis of (1)

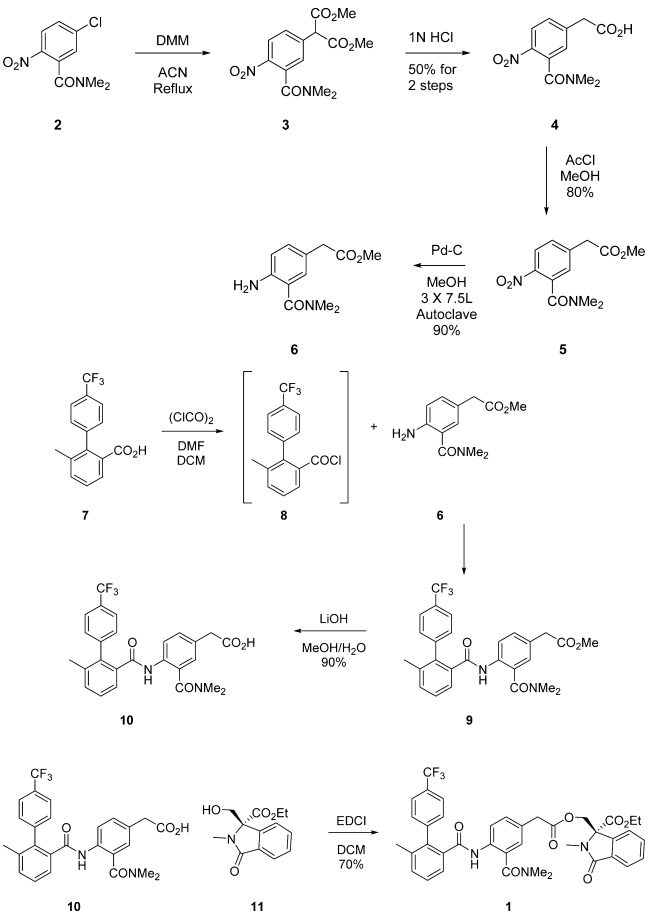

Scheme 2. Synthesis of intermediate (13)

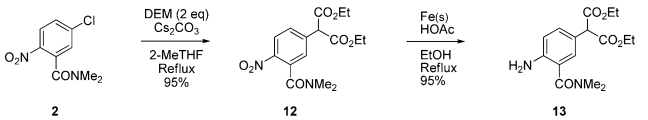

Special Issue: Process Analytical Technologies (PAT) 14

Received: October 9, 2014

dx.doi.org/10.1021/op5003165 | *Org. Process Res. Dev.* XXXX, XXX, XXX−XXX

Limited access to larger quantities of acid **7** through commercial sources necessitated the need to quickly develop a process to **7** (Scheme 3). Standard Suzuki coupling of aryl

Scheme 3. Synthesis of intermediate carboxylic acid (7)

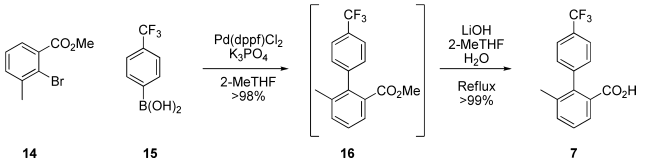

bromide (**14**) and boronic acid (**15**) followed by hydrolysis in a single pot afforded **7** as the crude acid.[2] The acid was purified via recrystallization from ethanol and water affording the acid (**7**) in excellent purity and yield. This process was sourced to multiple vendors who successfully prepared **7** in order to support the manufacturing campaign also described later herein.

The final component (**11**) was prepared utilizing a procedure similar to Othman and co-workers (Scheme 4).[3] Treatment of

Scheme 4. Synthesis of intermediate lactam (11)

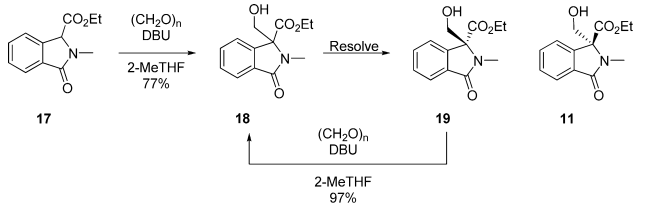

lactam **17** with paraformaldehyde generated racemic **18** in 77% isolated yield. Attempts were made to develop a classical resolution with promising initial results, however due to time constraints that process was not further optimized. Instead lactam (**18**) was resolved via simulated moving bed (SMB) chiral chromatography with recycling of the undesired enantiomer (**19**). This process allowed for an overall 56% conversion after one recycling protocol. With all components now readily available, the task of preparing carboxylic acid **10** was initiated (Scheme 5).

As was previously mentioned, multiple solvents were utilized within the original processing. Final processing was to be carried out exclusively in 2-MeTHF; unfortunately, upon

Scheme 5. Formation of core 10

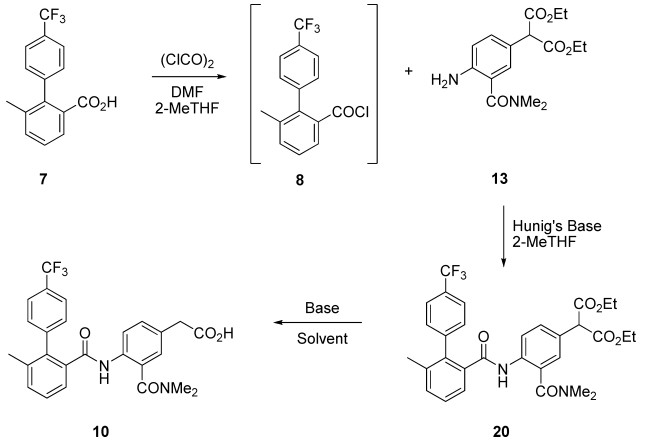

scaling the hydrolysis and decarboxylation (**20** → **10**), it was noted that significant amide hydrolysis occurred. The decomposition of **20** was presumably due to the increased solubility of acid (**10**) in 2-MeTHF exposed to strongly basic conditions. A variety of bases and solvents were investigated to determine optimal conditions (Table 1 and 2). Once K_2CO_3 had been determined to be an acceptable base for converting the ester (**20**) to the acid (**10**), we next looked into reducing overall processing time.

Table 1. Base effects on hydrolysis of 20 in refluxing 2-MeTHF

entry	base	time (hr)	yield
1	1 N LiOH	1	decomposition
2	1 N NaOH	1	decomposition
3	sat. $NaHCO_3$	24	N.R.
4	sat. K_2CO_3	18	>99%

Table 2. Solvent effects on hydrolysis of 20 with 2.5 equiv K_2CO_3(aq) at reflux

entry	solvent	time (hr)	yield
1	THF	1	>99%
2	MeOH	1	>99%
3	EtOH	3	>99%
4	2-MeTHF/MeOH	1	>99%

Although both THF and MeOH provided acceptable reaction times they brought with them processing complications. Ethanol avoided the formation of mixed esters and allowed for easy isolation by distillation of the solvent. Treatment of the product rich aqueous layer with HCl precipitated the desired acid **10** from solution. Thus, after three chemical transformations and recrystallization, (**10**) was isolated in 85% overall yield starting from (**7**).

Special care to wash **10** with excess water was required to purge any residual HCl. Recrystallization of acid **10** from toluene in the presence of HCl leads to the formation of **21**, presumably via activation of the dimethylamide followed by intramolecular cyclization (Scheme 6).

Scheme 6. Hydrolysis and lactonization of 10

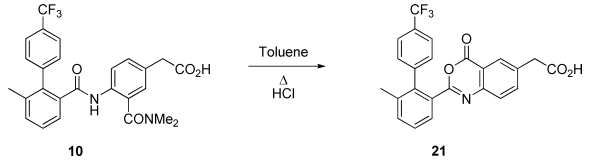

All that remained was coupling of acid **10** with lactam **11**. Esterification was previously conducted utilizing EDCI as the free base. A variety of alternatives were investigated (CDMT, EDCI, T3P, mixed anhydride, and acid chloride) including EDCI–HCl (Scheme 7).

While most coupling conditions provided the desired product, ultimately EDCI·HCl was selected. While stressing the reaction conditions, it was noted that a minor impurity started to develop. This impurity was isolated and characterized as the EDCI adduct (**22**). Formation of the impurity was readily managed by dose-controlled addition of EDCI·HCl to a mixture of both acid (**10**) and primary alcohol (**11**) minimizing significant changes in reaction temperatures. Following workup,

dx.doi.org/10.1021/op5003165 | Org. Process Res. Dev. XXXX, XXX, XXX–XXX

Scheme 7. Esterification of 10 to generate 1

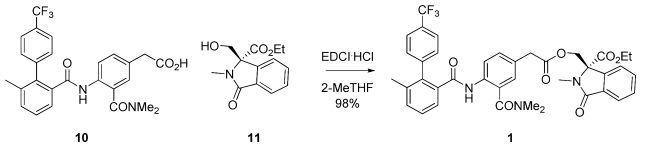

the crude materials were isolated in 98% purity and yield with no detectable EDCI adducts present. Unfortunately, the crude materials required purification via silica gel as a solid form isolation was unknown at the time. To further complicate isolation, the product (**1**) had exceptional solubility in all common solvents aside from heptanes and water. Thus, in order to isolate the API, the product-rich solutions were concentrated to a low volume and charged to an excess of water. The solids were ultimately isolated as an amorphous powder.

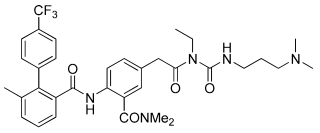

22

Reaction Monitoring. Online reaction monitoring tools such as mid-infrared (MIR), near-infrared (NIR), Raman, and NMR have found wider and wider use in API process development and other pharmaceutical development.[4−14] As several processing steps required the use of hazardous reagents (oxalyl chloride) or elevated temperatures (decarboxylation), ReactIR monitoring was extensively utilized to minimize worker exposure and reduce cycle time during the development and scale-up. In the lab-scale experiments, a REACT IR iC10 by Mettler Toledo AutoChem with a 6.5 mm AgX DiComp Fiber Conduit probe was used in reaction monitoring. Samples were also collected for off line UPLC end-point determination and for comparison to the ReactIR results. The ReactIR monitoring data were collected for major steps described in an early process development scheme (Scheme 1).

The reactions of formation of acid chloride (converting **7** to **8**), the subsequent coupling reaction (**8** and **13** to **20**), and the hydrolysis of **20** to **10** were all successfully monitored by ReactIR (Scheme 5). Since there were distinct IR absorption band(s) that can be assigned to either reactant or product in these reaction steps, three separate univariate models by iC IR software were established that can describe both consumption of a reactant and buildup of the product in each reaction. The ReactIR results correlated with off-line UPLC analysis results well.

Furthermore, monitoring the transformation of **10** and **11** to final product **1** highlights the power of ReactIR as a process monitoring tool (Scheme 7). In this specific step, there are multiple distinct carbonyls involved in the transformation, extracting the reaction progression information from the presence, formation, and or disappearance of these carbonyls is quite daunting (Figure 2). Early LC methods were complicated by overlapping peaks which relegated the team to letting the reaction progress for 18 h to ensure completion. The ReactIR monitoring data for this transformation were processed by iC IR software (ConcIRT module) to successfully build a multivariate model. This model simultaneously monitors the decrease of the key reactant **10** and increase of

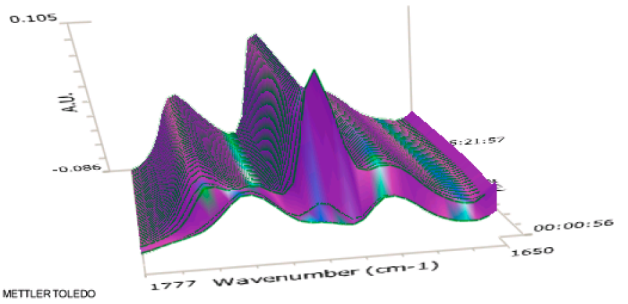

Figure 2. IR spectra changes as a function of reaction progression (time). 3-D surface plot of the spectra as a function of time and wavelength.

the product **1** (Figure 3). The ability of ReactIR to simultaneously track these reactants and products in real time

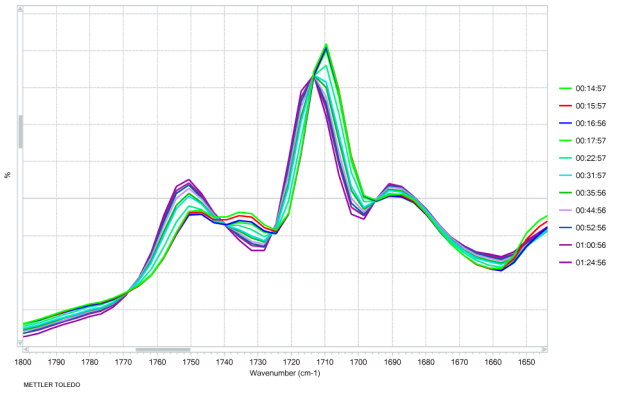

Figure 3. Overlay plot of the spectra at selected time points.

continuously allowed the team to determine that the reaction was ca. 75% complete within the first hour and >98% complete within 6 h (Figure 3), thus affording the team greater confidence in scaling.

In the subsequent process optimization experiments, ReactIR was continuously used to acquire online IR spectra along with a few samples for offline UPLC analysis. For the optimized reaction process (Scheme 5), we confirmed that reaction monitoring by ReactIR is still feasible for the reactions of formation of acid chloride (converting **7** to **8**) and the subsequent coupling reaction (**8** and **13** to **20**). Two univariate models were established for the two reactions. However, because of the changes in reagents and solvent that introduced spectrum interference, reaction monitoring by ReactIR was no longer possible for the conversion of **20** to **10**.

Monitoring the transformation of **10** and **11** to product **1** in the optimized process was still successful despite the change in solvent for the reaction. A careful examination of the ReactIR spectrum changes over time revealed that the subtle changes, mostly in the range of 1660 cm^{-1} to 1800 cm^{-1} that are related to band changes of the carbonyls, closely related to the reaction progression (Figure 2, bottom plot). Therefore, the online IR spectrum changes in this range were correlated to corresponding offline UPLC analysis results to build a quantitative multivariate model for accurately monitoring the reaction progression (Figure 4). The model was built in iCQuant module of the iC IR software. A multivariate mathematical technique—partial least squares (PLS)[15]—was used to relate the online IR measurements (e.g., spectra after applying second

dx.doi.org/10.1021/op5003165 | Org. Process Res. Dev. XXXX, XXX, XXX−XXX

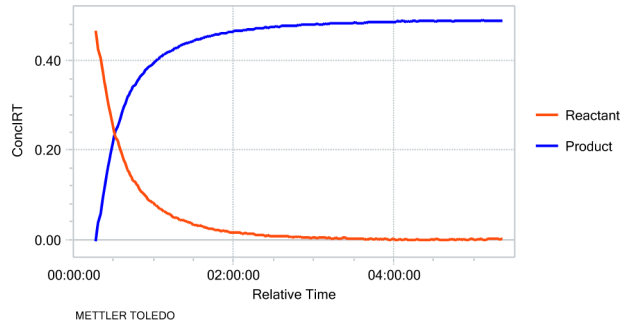

Figure 4. Reaction progression trends for the reactant and the product (**1**) in Scheme 5. The trends were obtained from ConcIRT multivariate analysis in iC IR software using a spectrum range of 900−1900 cm^{-1}.[5,6]

derivative) from a set of spectra over time in a reaction to the property value of interest − % conversion (reactant or product) obtained for the same reaction from offline LC testing. This set of sample was called the training set, and the resulting PLS model is described in Figure 5 in blue for the PLS model-

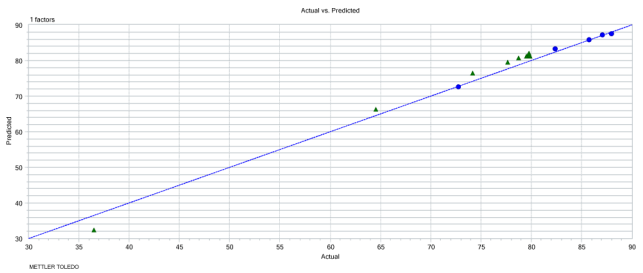

Figure 5. Quantitative multivariate model for accurately monitoring the reaction progression (product **1** formation) using the spectrum data in range of 1660 cm^{-1} to 1800 cm^{-1}. Blue data points were used to build the model from one set of online IR and corresponding offline UPLC data; the green data points were used to verify the validity of the model from another independent set of experiment.

predicted % conversion (predicted) vs the LC measured % conversion (actual). The blue points were the experimental points, and the blue line is the model-predicted linear correlation. Then, another set of data from reaction monitoring from another independent experiment was used to check the validity of the model. This set of data was described in the same plot in green for the PLS model predicted % conversion (predicted) vs the LC measured % conversion (actual). The agreement of the two sets of data is very good.

The model was successfully used to guide the process scale-up from lab scale all the way to a >10 kg scale in a pilot plant. Finally, the transformation of **10** and **11** to final product **1** in the pilot plant was monitored using a special online IR instrument: MonARC with an extended length IR probe from Mettler Toledo AutoChem. MonARC is designed for mid-infrared (FTIR) based process monitoring in classified area environments.

In conclusion, we have developed a six-step synthesis in 72% overall yield of (**1**) from three key components. Key developments include (i) simplified solvent scheme, (ii) improved processing and yields, (iii) elimination of multiple catalyst loadings, and (iv) ReactIR monitoring minimizing worker exposure and side products.

Experimental Section. All reactions were run in standard air-dried glassware with magnetic stirring under a static atmosphere of nitrogen unless otherwise noted. Mass spectral data were obtained on a Micromass ZMD mass spectrometer with flow injection analysis and atmospheric pressure chemical ionization (APCI). Reactions were monitored by Bruker 400 MHz ^{1}HNMR, Agilent 1290 UPLC, and REACT IR iC10 with 6.5 mm AgX DiComp fiber conduit probe by Mettler Toledo AutoChem. The REACT IR data were processed by iC IR version 4.0 by Mettler Toledo AutoChem. Commodity reagents were purchased from reputable vendors and used as received.

*2-(3-(Dimethylcarbamoyl)-4-(6-methyl-4′-(trifluoromethyl)-[1,1′-biphenyl]-2-carboxamido)phenyl)acetic Acid (**10**).* A 200 L glass lined tank equipped with ReactIR Probe (Mettler-Toledo Dicomp AgX probe (9.5 mm O.D. × 29 in. long, 2 m AgX fiber)) and scrubber was purged with nitrogen and charged with 2-methyltetrahydrofuran (80.0 L, 10 L/kg) and 6-methyl-4′-(trifluoromethyl)-[1,1′-biphenyl]-2-carboxylic acid (**7**) (8.0 kg, 28.6 mol, 1.0 equiv) followed by initiating stirring. After 20 min of stirring at 20 ± 5 °C, DMF (0.02 L, 0.29 mol, 0.02 equiv) was charged followed by addition of oxalyl chloride (3.99 kg, 31.4 mol, 1.10 equiv) while maintaining a temperature of 20 ± 5 °C. After 2 h the trending plot of the ReactIR spectrum changes over time (univariate model) indicated that the reaction is essentially complete with an IPC confirming <2% residual **7** present. Excess oxalyl chloride was purged by distillation/replacement of 2-MeTHF (12.0 L total). The tank was cooled to 0 °C followed by the addition of diethyl 2-(4-amino-3-(dimethylcarbamoyl)phenyl)malonate (**13**) (9.29 kg, 28.8 mol, 1.01 equiv) over 15 min while maintaining a temperature of 5 ± 5 °C. Diisopropylethylamine (7.42 L, 42.5 mol, 1.49 equiv) was charged such that the internal temperature remains at 10 ± 15 °C. Upon complete addition, the reaction mixture was warmed to 20 °C. After 1 h the trending plot of the ReactIR spectrum changes over time (univariate model), indicating that the reaction is essentially complete with an IPC confirming <2% residual 6-methyl-4′-(trifluoromethyl)-[1,1′-biphenyl]-2-carbonyl chloride (**8**) present. 1 N Hydrochloric acid (60.0 L) was charged to the slurry followed by 30 min of agitation. Stirring was stopped where upon the layers separated. The heavy aqueous layer was disposed of followed by washing the organic layer with water (40.0 L) and an additional 30 min of agitation. The scrubber was removed from the reaction train followed by concentration of the organic layers containing diethyl 2-(3-(dimethylcarbamoyl)-4-(6-methyl-4′-(trifluoromethyl)-[1,1′-biphenyl]-2-carboxamido)phenyl)-malonate (**20**) to ca. 50.0 L under vacuum while maintaining a temp of 25 ± 10 °C. Once distillation was complete, the temperature was set to 20 ± 5 °C followed by addition of 1 N potassium carbonate (80.0 kg) and ethanol (40.0 L). The entire mixture was heated to reflux (75 ± 10 °C) over 2 h to avoid any potential excessive off-gassing. The mixture was held for 15 h with the IPC confirming <2% residual **20** present. The mixture was cooled to 20 °C followed by removal of the heavy aqueous phase. The product rich organic layer was concentrated to ca. half the initial volume (50.0 L) under vacuum while maintaining a 35 ± 10 °C. The displaced solvent was then replaced with additional 2-MeTHF (65 L) via constant volume displacement under vacuum while maintaining a 35 ± 10 °C. Once the ethanol levels were acceptable (<5%), the temperature was adjusted to 20 °C. To the cooled organic solution was charged 80.0 L of 1 N NaOH followed by 5 min of

dx.doi.org/10.1021/op5003165 | Org. Process Res. Dev. XXXX, XXX, XXX−XXX

agitation and settling. The product-rich aqueous layer was collected followed by disposal of the top organic layer. To the product rich aqueous layer was added 2 N HCl until the pH was 1−2. The product precipitated from solution when the pH reached ∼4; however, additional HCl was charged to increase product recovery. The solids were isolated via filtration followed by rinsing with water (160.0 L). After 24 h of drying over forced air, crude **10** (13.0 kg) was isolated. The crude materials were subsequently recrystallized from toluene (15.0 L/kg), affording 11.8 kg of **10** in 85% yield over three steps.

*Ethyl-(R)-1-((2-(3-(dimethylcarbamoyl)-4-(6-methyl-4′-(trifluoromethyl)-[1,1′-biphenyl]-2-carboxamido)phenyl)acetoxy)methyl)-2-methylisoindoline-1-carboxylate (**1**).* A 200 L glass lined tank equipped with ReactIR probe was purged with nitrogen and charged with 2-methyltetrahydrofuran (65.0 L, 15 L/kg), ethyl (*R*)-1-(hydroxymethyl)-2-methyl-3-oxoisoindoline-1-carboxylate (**11**) (4.3 kg, 17.3 mol, 1.0 equiv), carboxylic acid **10** (9.2 kg, 19.0 mol, 1.1 equiv), and DMAP (0.4 kg, 3.45 mol, 0.2 equiv). The initial slurry was held at 20 ± 5 °C for 30 min or until the solids had completely dissolved. To the solution was charged in 5 portions EDCI·HCl (4.1 kg, 21.6 mol, 1.25 equiv) while maintaining a batch temperature of 20 ± 5 °C. After 7 h the trending plot of the ReactIR spectrum changes over time (multivariate model, Figure 2) indicated the reaction was complete. To the vessel was charged 1 N HCl (70.5 L) followed by 30 min of agitation. The heavy aqueous layer was removed followed by charging 70.5 L of sat. $NaHCO_3$ (caution should be used to avoid any excessive off-gassing). The heavy aqueous layer was removed followed by a second wash of $NaHCO_3$ (75.0 L). The biphasic mixture was agitated for 30 min followed by removal of the heavy aqueous layer. The remaining product-rich organic layer was concentrated to a lowest stirrable volume followed by dilution with toluene (10 L/kg).

The toluene mixture was submitted to large-scale silica gel purification where the desired materials were isolated from acetone/toluene. The product rich material was concentrated to lowest stirrable volume followed by dilution in EtOAc (azeatrope acetone) followed by EtOH (azeatrope EtOAc/toluene) To a 200 L glass lined reactor charged with 151 L of water (2 ± 2 °C) was added the product-rich EtOH solution (∼15 L) through a 5 μ in-line filter over an hour. After an hour of granulation, **1** (10.8 kg, 15.1 mol, 88%) was isolated by filtration.

Data: ^{1}H NMR (700 MHz, MeOD d_4): 7.74 (d, 2H, 7.5 Hz), 7.68 (d, 1H, 7.5 Hz), 7.55 (m, 4H), 7.47 (m, 4H), 7.10 (d, 1H, 8.0 Hz), 6.97 (s, 1H), 6.93 (d, 1H, 8.0 Hz), 4.91 (d, 1H, 12 Hz), 4.78 (d, 1H, 12 Hz), 4.20 (m, 1H) 4.12 (m, 1H), 3.44 (s, 2H), 3.04 (s, 3H), 3.02 (s, 3H), 2.84 (s, 3H), 2.15 (s, 3H), 1.17 (t, 3H, 7.3 Hz); ^{13}C NMR (700 MHz, MeOD d_4): 171.45, 171.41, 170.76, 170.74, 168.77, 144.65, 142.20, 139.23, 138.45, 137.97, 134.84, 133.60, 133.07, 132.64, 132.32, 131.85, 131.45, 131.21, 130.95, 130.45, 129.59, 129.19, 126.18, 126.00, 125.94, 125.79, 124.56, 123.43, 72.72, 64.22, 63.97, 40.73, 40.10, 35.51, 27.18, 20.64, 14.30; HRMS (ESI $C_{39}H_{37}F_3N_3O_7$) calc 716.2478 u, found 716.2582 u.

AUTHOR INFORMATION

Corresponding Author

*E-mail: Shane.a.Eisenbeis@pfizer.com.

Notes

The authors declare no competing financial interest.

ACKNOWLEDGMENTS

The authors gratefully acknowledge Jeff Sperry, Roger Ruggeri, and Edward Conn for helpful discussions, as well as Barb Sitter for assistance with DoE studies in support of the conversion of **10** to **1** and Ling Zhang for data analysis by PLS modeling.

REFERENCES

(1) *Handbook of Green Chemistry*, Vol. 2 Green Catalyst; Anastas, P. T., Ed.; John Wiley and Sons: New York, 2012.
(2) Suzuki, A.; Miyaura, N. *Chem. Rev.* **1995**, *95*, 2457−2483.
(3) Othman, M.; Decroix, B. *Syn. Comm.* **1996**, *26* (12), 2803. Othman, M.; Decroix, B.; Pigeon, P. *Tetrahedron* **1998**, *54* (30), 8737. Roche, B.; Conn, E.; Eisenbeis, S.; Ruggeri, R. *Tetrahedron Lett.* **2012**, *53* (41), 5467−5470.
(4) Chen, R.; Bowles, D.; Antosz, F.; Xiang, Y.; Li, S.; Barrila, M.; Coutant, M. Practical Approaches in Applying Process Analytical Technology (PAT) Tools for Early API Development. *Pharmaceutical Outsourcing*, August/September **2011**, 28−33.
(5) Zhou, G.; Guenard, R.; Ge, Z. Infrared and Raman spectroscopy for process development. In *Applications of Vibrational Spectroscopy in Pharmaceutical Research and Development*; Pivonka, D. E., Chalmers, J. M., Griffiths, P. R., Eds.; Wiley: New York, 2007; pp 185−211.
(6) Chanda, A.; Daly, A. M.; Foley, D. A.; Lapack, M. A.; Mukherjee, S.; Orr, J. D.; Reid, G. L.; Thompson, D.; Howard, W. Industry Perspectives on Process Analytical Technology: Tools and Applications in API Development. *Org. Process Res. Dev.*, 10.1021/op400358b.
(7) Sistare, F.; Laurie, P. B., St.; Mojica, C. A. Process Analytical Technology: An Investment in Process Knowledge. *Org. Process Res. Dev.* **2005**, *9* (3), 332−336.
(8) Lin, Z.; Zhou, L.; Mahajan, A.; Song, S.; Wang, T.; Ge, Z.; Ellison, D. Real-time endpoint monitoring and determination for a pharmaceutical salt formation process with in-line FT-IR spectroscopy. *J. Pharm. Biomed. Anal.* **2006**, *41* (1), 99−104.
(9) Conlon, D. A.; Izzo, B.; Collins, P. Mid-infrared monitoring applications during development of the vinyl ether formation step in the preparation of aprepitant. *Process Chemistry in the Pharmaceutical Industry*; Gadamasetti, K., Braish, T., Eds.; CRC Press: Boca Raton, FL, 2008; pp 349−360.
(10) Smith-Goettler, B.; Bakeev, K. A. On-line PAT applications of spectroscopy in the pharmaceutical industry. In *Process Analytical Technology*, 2nd ed.; Wiley: New York, 2010; pp 439−461.
(11) Carter, C. F.; Lange, H.; Ley, S. V.; Baxendale, I. R.; Wittkamp, B.; Goode, J. G.; Gaunt, N. L. ReactIR Flow Cell: A new analytical tool for continuous flow chemical processing. *Org. Process Res. Dev.* **2010**, *14* (2), 393−404.
(12) Csontos, I.; Pataki, H.; Farkas, A.; Bata, H.; Vajna, B.; Nagy, Z. K.; Keglevich, G.; Marosi, G. J. Feedback Control of Oximation Reaction by Inline Raman Spectroscopy. *Org. Process Res. Dev.* **2014**, 10.1021/op500015d.
(13) Foley, D. A.; Wang, J.; Maranzano, B.; Zell, M. T.; Marquez, B. L.; Xiang, Y.; Reid, G. L. Online NMR and HPLC as a Reaction Monitoring Platform for Pharmaceutical Process Development. *Anal. Chem.* **2013**, *85* (19), 8928−8932.
(14) Calow, A. D. J.; Carbo, J. J.; Cid, J.; Fernandez, E.; Whiting, A. Understanding α,β-Unsaturated Imine Formation from Amine Additions to α,β-Unsaturated Aldehydes and Ketones: An Analytical and Theoretical Investigation. *J. Org. Chem.* **2014**, *79* (11), 5163−5172.
(15) Esbensen, K. H. *Multivariate Data Analysis - In Practice An Introduction to Multivariate Data Analysis and Experimental Design*, 5th ed.; CAMO Software: Woodbridge, NJ, 2010.